Sodium Iodate Produces a Strain-Dependent Retinal Oxidative Stress Response Measured In Vivo Using QUEST MRI

Bruce A. Berkowitz,[1,2] Robert H. Podolsky,[3] Jacob Lenning,[1] Nikita Khetarpal,[1] Catherine Tran,[1] Johnny Y. Wu,[1] Ali M. Berri,[1] Kristin Dernay,[1] Fatema Shafie-Khorassani,[3] and Robin Roberts[1]

[1]Department of Anatomy and Cell Biology, Wayne State University School of Medicine, Detroit, Michigan, United States
[2]Department of Ophthalmology, Wayne State University School of Medicine, Detroit, Michigan, United States
[3]Deptarment of Family Medicine and Public Health Sciences, Wayne State University, Detroit, Michigan, United States

Purpose. We identify noninvasive biomarkers that measure the severity of oxidative stress within retina layers in sodium iodate (SI)-atrophy vulnerable (C57BL/6 [B6]) and SI-atrophy resistant (129S6/SvEvTac [S6]) mice.

Methods. At 24 hours after administering systemic SI to B6 and S6 mice we measured: (1) superoxide production in whole retina ex vivo, (2) excessive free radical production in vivo based on layer-specific 1/T1 values before and after α-lipoic acid (ALA) administration while the animal was inside the magnet (QUEnch-assiSTed MRI [QUEST MRI]), and (3) visual performance (optokinetic tracking) ± antioxidants; control mice were similarly assessed. Retinal layer spacing and thickness in vivo also were evaluated (optical coherence tomography, MRI).

Results. SI-treated B6 mice retina had a significantly higher superoxide production than SI-treated S6 mice. ALA-injected SI-treated B6 mice had reduced 1/T1 in more retinal layers in vivo than in SI-treated S6 mice. Uninjected and saline-injected SI-treated B6 mice had similar transretinal 1/T1 profiles. Notably, the inner segment layer 1/T1 of SI-treated B6 mice was responsive to ALA but was unresponsive in SI-treated S6 mice. In both SI-treated strains, antioxidants improved contrast sensitivity to similar extents; antioxidants did not change acuity in either group. Retinal thicknesses were normal in both SI-treated strains at 24 hours after treatment.

Conclusions. QUEST MRI uniquely measured severity of excessive free radical production within retinal layers of the same subject. Identifying the mechanisms underlying genetic vulnerabilities to oxidative stress is expected to help in understanding the pathogenesis of retinal degeneration.

Keywords: QUEST MRI, free radicals, reactive oxygen species, strain, sodium iodate

Preventing or slowing progression of sight-threatening outer retinal degeneration resulting from, for example, genetic disease remains challenging. Clinical and experimental studies have implicated outer retinal oxidative stress in the pathology of many forms of outer retinal degeneration.[1–20] Yet, it remains unclear as to whether antioxidants (AOs) confer a benefit against photoreceptor atrophy in patients.[6,7,21] This uncertainty is likely due, in part, to a limited ability to objectively determine effective reduction of regional retinal oxidative stress in patients after AO treatment.[6,7,21] Thus, there is a pressing need for new methods that will measure the severity of excessive free radical production in different layers of the retina in vivo and have translational potential.

New noninvasive biomarkers to address this problem have been suggested. Excessive free radical production can be detected in vivo without a contrast agent using QUEnch-assiSTed magnetic resonance imaging (QUEST MRI).[22–24] The QUEST MRI index evaluates an abnormally high production of paramagnetic free radicals as a greater-than-normal spin-lattice

relaxation rate R1 (1/T1) that can be returned to baseline with an AO (i.e., a quench).[22–24] In MRI, nuclear spins (usually protons) are brought to a higher energy state with a radiofrequency pulse. The spin–lattice relaxation time ("T1") is a "life-time" measurement describing how quickly nuclear spins return back to their equilibrium position along the direction of the static magnetic field while releasing energy to their surroundings (the "lattice"). Paramagnetic agents have unpaired electrons (e.g., Gd-DPTA, manganese, or free radicals) and shorten T1 causing R1 to increase linearly based on the concentration of the paramagnetic agent.[25] We have validated rod photoreceptor compartment-specific QUEST MRI measurements in vivo against a "gold standard" free radical assay ex vivo in several animal models.[22–24] Another promising noninvasive approach is optokinetic tracking (OKT), which measures cone-based visual performance and is sensitive to retinal oxidative stress.[26–30] While QUEST MRI and OKT detect the presence of oxidative stress in vivo, whether they can measure its severity remains unclear.

Administration of an oxidizing agent is a useful test of how well the retina can tolerate oxidative stress.[2,17,20,26,31–33] Low doses of sodium iodate (SI) are reported to produce more outer retinal atrophy on histologic examination in B6 mice than in S6 mice.[2,23,31,32] Thus, we hypothesized that before overt atrophy, SI-treated B6 mice experience more outer retinal oxidative stress than SI-treated S6 mice.

In this study, we tested this hypothesis using a low dose of SI.[23] Superoxide production was measured from ex vivo retinas as a "gold standard" outcome.[34,35] We evaluated sustained production of abnormally high levels of inherently paramagnetic free radicals, which are MRI 1/T1 contrast agents,[22–24] in different retinal layers of each mouse before and after in-magnet injection of either saline or α-lipoic acid (ALA; QUEST MRI).[22,23] ALA is a relatively fast-acting, potent free radical scavenger that normally is found in mitochondria and that readily crosses blood–neuron barriers.[36,37] Furthermore, OKT assessment of visual performance with and without administration of methylene blue (MB) + ALA (our previously described AO cocktail) was evaluated.[22,23,26,27] MB is a "parasitic" electron transporter widely reported to correct mitochondrial- and oxidase-induced oxidative stress.[38,39] Finally, retinal layer spacing and thicknesses were noninvasively examined using optical coherence tomography (OCT) and MRI.[22,23]

MATERIALS AND METHODS

All animals were treated in accordance with the National Institutes of Health (NIH; Bethesda, MD, USA) Guide for the Care and Use of Laboratory Animals, the Association for Research in Vision and Ophthalmology (ARVO) Statement for the Use of Animals in Ophthalmic and Vision Research, and Institutional Animal and Care Use Committee authorization. Animals were housed and maintained in 12-hour:12-hour light-dark cycle laboratory lighting unless otherwise noted. Mice were euthanized by humanely cervical dislocation followed by a bilateral pneumothorax, as detailed in our IACUC-approved protocol.

Groups

Male 2- to 3-month-old C57BL/6 (B6, Jackson Laboratory, Bar Harbor, ME, USA) and 129S6/SvEvTac (S6, Taconic Biosciences, Hudson, NY, USA) mice were studied. Approximately 24 hours before examination, mice of both strains were injected with SI dissolved in saline (bolus intraperitoneal [IP], 20 mg/kg; Sigma-Aldrich Corp., St. Louis, MO, USA). This dose and time point produced outer retinal oxidative stress without substantial outer retinal degeneration in atrophy-vulnerable (C57BL/6 [B6]) mice.[17,23,32]

Retinal Superoxide Production

Subgroups of dark-adapted B6 and S6 mice were treated with SI. These mice were maintained in darkness for at least 16 hours before euthanasia and retina removal. Superoxide production was measured on each retina using a standard lucigenin (bis-N-methylacridinium nitrate; Sigma-Aldrich Corp.).[23]

QUEST MRI Evaluation

Subgroups of mice were maintained in darkness for at least 16 hours before and during the MRI examination. In all groups, immediately before the MRI experiment, animals were anesthetized with urethane (36% solution IP; 0.083 mL/20 g animal weight, prepared fresh daily; Sigma-Aldrich Corp.) and treated topically with 1% atropine sulfate (Akorn Pharmaceuticals, Lake Forest, IL, USA) to ensure dilation of the iris. This is

followed by 3.5% lidocaine gel (Akorn Pharmaceuticals) to reduce sensation that might trigger eye motion and to keep the ocular surface moist. Also, an IP catheter (Terumo Surflo, 24ga, 0.75 inches; Thermo Fisher Scientific, Waltham, MA, USA) was positioned and secured intraperitoneally for injections inside the magnet. High resolution 1/T1 data were acquired on a 7T system (Bruker ClinScan, Billerica, MA, USA) using a receive-only surface coil (1.0 cm diameter) as regularly performed in our laboratory.[22,23,40] In all cases, several single spin-echo (time to echo [TE] 13 ms, 7×7 mm², matrix size 160×320, slice thickness 600 μm, in-plane resolution 21.875 μm) images were acquired at different repetition times (TRs) in the following order (number per time between repetitions in parentheses): TR 0.15 seconds (6), 3.50 seconds (1), 1.00 seconds (2), 1.90 seconds (1), 0.35 seconds (4), 2.70 seconds (1), 0.25 seconds (5), and 0.50 seconds (3). To compensate for reduced signal-to-noise noise ratios at shorter TRs, progressively more images were collected as the TR decreased. 1/T1 data were collected before (i.e., baseline) and 13 and 29 minutes (the middle time points of the image acquisitions) after acute saline (10 μL/g) or ALA (50 mg/kg, dissolved in saline and pH adjusted to approximately 7.4) injection inside the magnet. To improve the signal-to-noise ratio, data collected at 13 and 29 minutes after either ALA or saline administration were averaged.

OKT Evaluation

Two visual performance metrics were evaluated 24 hours after SI injection in dark-adapted, awake, and freely moving mice: spatial frequency thresholds (SFT, "acuity," in cycles/deg [c/d]) and contrast sensitivity (CS, measured at the peak of the nominal curve [0.06 cycles/deg], inverse Michelson contrast [unitless]) using the OKT reflex (OptoMotry, CerebralMechanics, Inc., Alberta, Canada) as described previously.[41] In brief, a vertical sine wave grating is projected as a virtual cylinder in three-dimensional coordinate space on computer monitors arranged in a quadrangle around a testing arena. Unrestrained mice (after an overnight dark adaptation) are placed on an elevated platform at the center of the arena. An experimenter used a video image of the arena from above to view the animal and follow the position of its head with the aid of a computer mouse and a crosshair superimposed on the mouse head. The X–Y positional coordinates of the crosshair are centered on the hub of the virtual cylinder, enabling its wall to be maintained at a constant "distance" from the animal's eyes, and thereby adjusting the spatial frequency (SF) of the stimulus to a fixed viewing position. When the cylinder was rotated in the clockwise (CW) or counter clockwise (CCW) direction and the animal followed with head and neck movements that tracked the rotation, it was judged whether the animal's visual system could distinguish the grating. CW and CCW tracking provides a measure of left and right eye SFT and CS.[41,42] One set of SFT and peak of CS measurements can reliably be obtained in 30 minutes.[42] Control mice, and SI-treated B6 and S6 mice ± MB+ALA (an AO cocktail that corrected excessive free radical production in the SI model[22,23]) were evaluated to investigate the contribution of excessive free radicals to visual performance indices. The OKT operator was blinded to the condition (SI-treated or SI-treated + AO) of the mice.

OCT Evaluation

OCT (Envisu R2200 VHR SDOIS) was used to visualize retinal layer spacing in vivo in subsets of mice ($n = 2$ per group). Mice were anesthetized with urethane (36% solution intraperitoneally; 0.083 mL/20 g animal weight, prepared fresh daily; Sigma-Aldrich Corp.). 1% atropine sulfate was used to dilate and
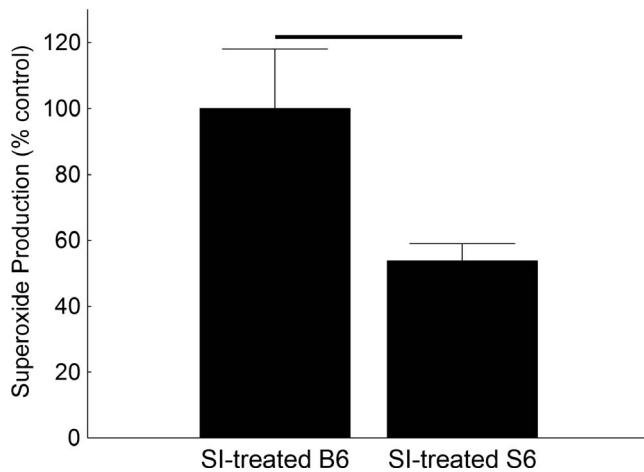
FIGURE 1. Excessive free radical production is greater in SI-treated B6 retina compared to that of SI-treated S6 retina. Superoxide production measured on the same day from excised retinas of dark-adapted SI-treated S6 ($n = 5$) and B6 ($n = 5$) mice. *Black bar*: significant difference ($P < 0.05$).

GenTeal was used to lubricate the eyes. OCT images also were used to visualize possible SI-evoked damage, and to spatially calibrate the transretinal MRI profiles.[43]

MRI Data Analysis

Within each T1 data set of 23 images, images acquired with the same TR were first registered (rigid body) and then averaged to generate a stack of 8 images. These averaged images then were registered across TRs. It is well known that using imperfect slice profiles leads to a bias in the estimate of T1 and a lower than expected T1 value (Chapter 18 in the book by Haacke et al.[44]). By normalizing to the shorter TR some of the bias can be removed giving a more accurate estimate for T1. We normalized by first applying 3×3 Gaussian smoothing (performed three times) on only the TR 150 ms image to minimize noise and emphasize signal. The smoothed TR 150 ms image then was divided into the rest of the images in that T1 data set. Preliminary experiments (not shown) found that this procedure help minimize the day-to-day variation in the 1/T1 profile previously noted and obviated the need for a "vanilla control" group used previously for correcting for day-to-day variations.[22,23] 1/T1 maps were calculated using the 7 normalized images via fitting to a three-parameter T1 equation ($y = a + b^*[\exp(-c^*TR)]$, where a, b, and c are fitted parameters) on a pixel-by-pixel basis using R (v.2.9.0; R Development Core Team. R: A language and environment for statistical computing. R Foundation for Statistical Computing, Vienna, Austria. ISBN 3-900051-07-0; 2009) scripts developed in-house, and the minpack.lm package (v.1.1.1; Elzhov TV, Mullen KM. Mullen minpack.lm: R interface to the Levenberg-Marquardt nonlinear least-squares algorithm found in MINPACK. R package version 1.1–1).

In each mouse, retinal thicknesses (µm) were objectively determined using the "half-height method" wherein a border is determined via a computer algorithm based on the crossing point at the midpoint between the local minimum and maximum, as detailed previously.[45,46] Thus, the distance between two neighboring crossing-points represents an objectively defined retinal thickness. 1/T1 profiles in each mouse then were normalized with 0% depth at the presumptive vitreoretinal border and 100% depth at the presumptive retina–choroid border. The present resolution is sufficient for extracting meaningful layer-specific anatomical and functional data, as discussed previously.[36,42]

Statistical Analysis

Data are presented as mean ± SEM. All superoxide, OKT, and MRI thicknesses measurements were evaluated for a normal distribution. Superoxide levels were compared using an unpaired *t*-test. All OKT indices had a normal distribution, and comparisons were performed using a 1-way ANOVA. MRI thickness measurements were compared using the Kruskal-Wallis test (nonparametric 1-way ANOVA); this nonparametric test was used because the low n in some groups precluded determination of a normal distribution. For the MRI profile data, we used a linear mixed model with cubic splines to model and compare mouse-specific profiles between groups. The number of "windows" with a relationship between 1/T1 and location (i.e., "knots") initially was evaluated separately for each group for any given analysis, and the Akaike and Schwarz Bayesian information criteria (AIC and BIC) were used to identify the model with the fewest knots needed to model all groups. Random coefficients for the intercept and location-specific coefficients (cubic spline coefficients) also were evaluated using AIC and BIC. The model included the fixed effects of strain, AO treatment, location-specific values for the cubic splines, and up to three-way interactions among the main effects. Higher-order interactions were removed from the model if they were not significant at the 0.05 level. To calculate a total AO effect across the entire profile, we summed the predicted values for the appropriate interaction across all locations. A significance level of 0.05 was used for all analyses.

RESULTS

Retinal Superoxide Production Ex Vivo

Compared to SI-treated B6 retina, SI-treated S6 retina had a 54% lower production of superoxide free radicals (Fig. 1).

QUEST MRI In Vivo

SI produced a greater-than-normal 1/T1 in the outer retina of B6 mice (compare black lines in Figs. 2A, 2B, 3A); these data are consistent with our previous report and with the sustained production of free radicals.[23] In SI-treated B6 mice, in-magnet injection of ALA (but not saline) decreased 1/T1 in the entire outer retina (44%–100%), in-line with quenching of excessive free radical production (Figs. 3A, 4A).[23] In SI-treated B6 mice, ALA also significantly reduced 1/T1 locally in the inner retina (16%–28% depth; Figs. 3A, 4A). In contrast, an ALA response was found in select regions of the outer retina of SI-treated S6 mice (48%–76%, and 88%–100%), and no response to ALA was observed in the inner retina (Fig. 4B). In other words, SI-treated B6 mice showed evidence in vivo of excessive free radical production in a larger portion of the retina than seen in SI-treated S6 mice (Fig. 4). Summation of the ALA response in the ALA-responsive regions revealed a 53% decrease in severity of free radical production mostly in the rod-dominated outer retina in SI-treated S6 versus SI-treated B6 mice (Fig. 4C), in agreement with the 54% decrease observed in the "gold standard" assays (Fig. 1).

OKT Evaluation

SFT did not change in either SI-treated B6 or SI-treated S6 mice with AO (Figs. 5A, 5C). However, CS significantly increased in both groups following treatment with AO, consistent with the presence of oxidative stress in cone cells (see discussion; Figs. 5B, 5D).
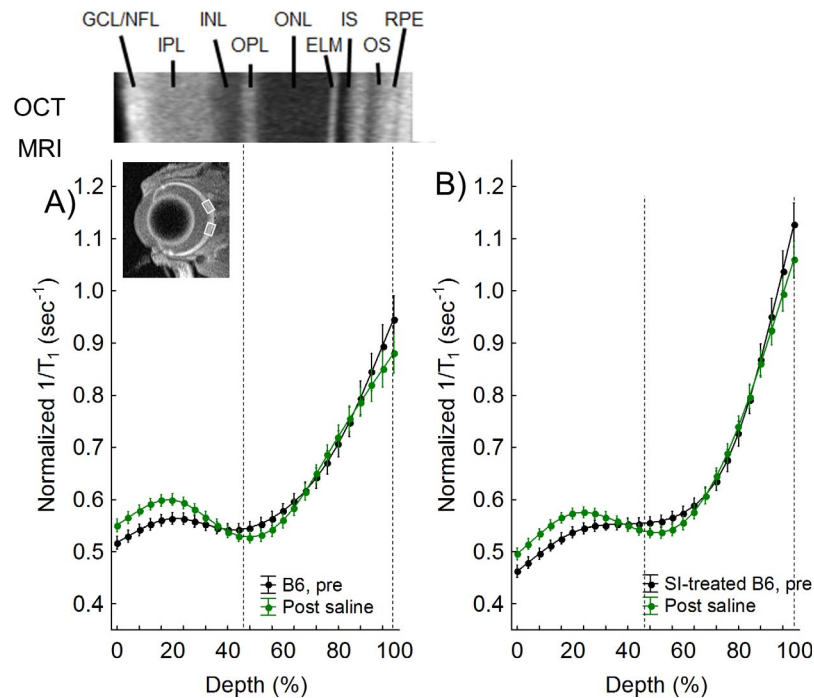
FIGURE 2. QUEST MRI measurements in B6 controls. Modelling results of normalized 1/T1 MRI profiles in vivo for the following groups (see Methods for details). (**A**) Dark-adapted C57Bl/6 (B6) group (*black*, $n = 3$) versus its paired profile after administration of saline inside the magnet (*green*). (**B**) Dark-adapted B6 mice treated 24 hours earlier with sodium iodate (*black*, $n = 4$) versus its paired profile after in-magnet administration of saline (*green*). Representative OCT image (above [**A**]) illustrate laminar spacing within the retina; layer assignments (GCL, ganglion cell layer; INL, inner nuclear layer; IPL, inner plexiform layer; IS, rod inner segment layer; OLM, outer limiting membrane; ONL, outer nuclear layer; OPL, outer plexiform layer; OS, rod outer segment layer) are as reported previously.[60] *Dashed vertical lines* map OPL (42%) and retina/choroid boundary (100%) onto MRI profiles (*below*). Retinal depth range with significant difference ($P < 0.05$) based on paired differences (e.g., Fig. 3). Each 1/T1 data set was normalized to its TR 150 ms image ("Normalized 1/T1"), as detailed in the Methods section.

Retinal Anatomy

In OCT images from representative mice, no evidence for retinal thinning was evident by visual inspection of the retinal layer spacing's between groups (Fig. 6A). In support of this observation, measurement of whole retinal thicknesses (MRI) found no differences between any groups (95% confidence intervals [CIs], B6 [221, 233 µm]; SI-treated B6 [213, 239 µm];
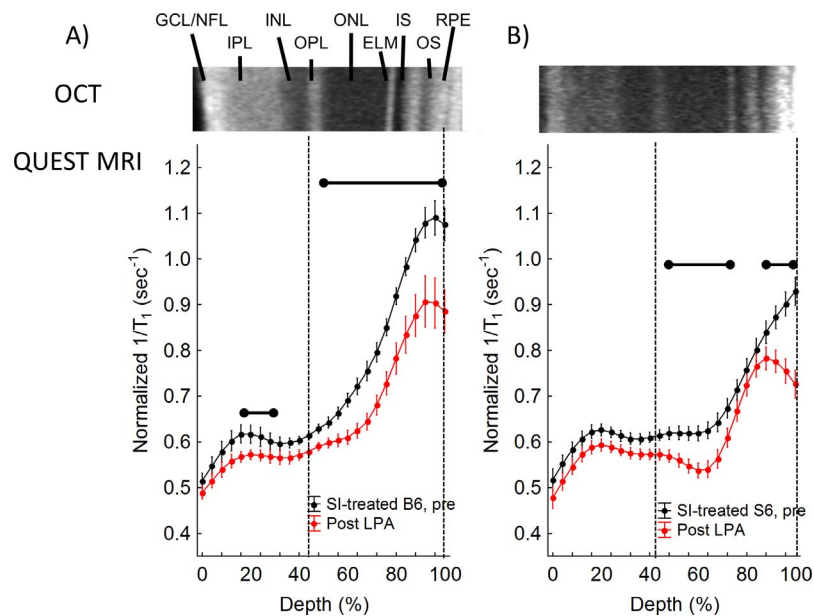

FIGURE 3. QUEST MRI measurements of SI-treated B6 mice. Modelling results of normalized 1/T1 MRI profiles in vivo (see Methods for details) for (**A**) SI-treated B6 (*black*, $n = 8$) and SI-treated B6+ALA (*red*, $n = 8$), and (**B**) SI-treated S6 (*black*, $n = 4$) and SI-treated S6+ALA (*red*, $n = 4$) groups. Other graphing conventions are detailed in Figure 2. Statistically significant differences are based on analysis of the difference plots presented in Figure 4.
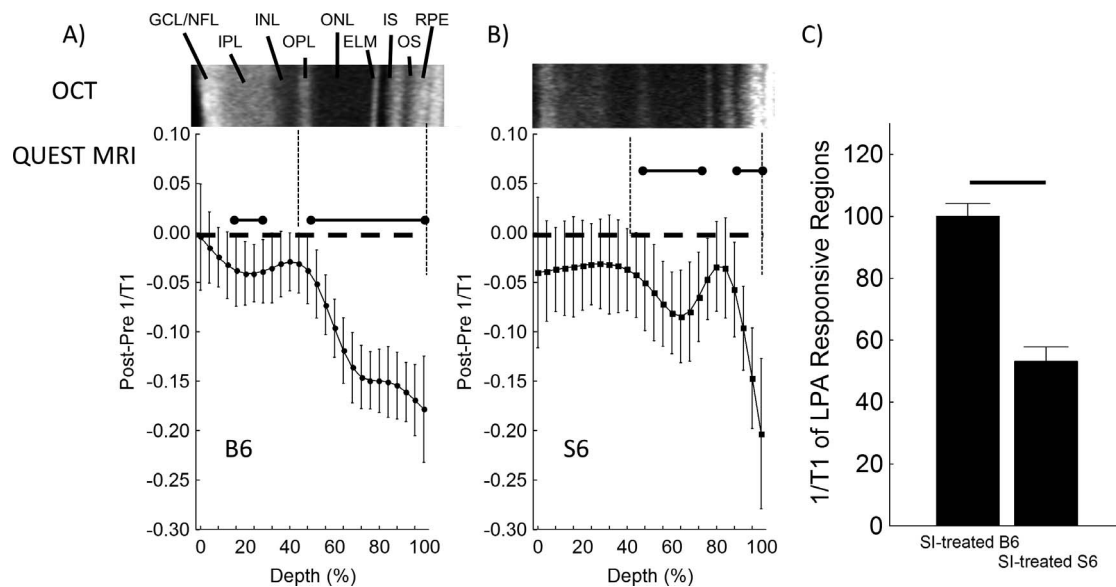
FIGURE 4. Difference QUEST MRI measurements in SI-treated B6 and SI-treated S6 mice. Modelling results of differences in normalized 1/T1 MRI profiles in vivo (see Methods for details) for (**A**) SI-treated B6 ($n = 8$) and (**B**) SI-treated S6 ($n = 4$) groups. Difference transretinal 1/T1 profiles were generated for each mouse by subtracting the normalized baseline 1/T1 at each location ("pre") from the normalized post ALA 1/T1; these then were averaged for the group. *Error bars*: 95% CIs. Graphing conventions are detailed in Figure 2. (**C**) Summary of positive ALA responsive regions in dark-adapted SI-treated B6 and SI-treated S6 mice as measured by QUEST MRI are in agreement with both conventional ex vivo assays (Fig. 1).

SI-treated B6+vehicle [198, 242 µm]; SI-treated B6+AO [204, 261 µm]; S6 [215, 229 µm]; SI-treated S6 [198, 226 µm]; SI-treated S6+vehicle [187, 246 µm]; SI-treated S6+AO [207, 244 µm]; Fig. 6B).

DISCUSSION

To our knowledge, our results provide a first-time demonstration that QUEST MRI measures the severity of sustained greater-than-normal production of free radicals within the outer retina of the same subject in vivo.[22,23] S6 and B6 strains were examined in our study based on reports that low doses of SI produce substantially less outer retinal damage in S6 mice than in B6 mice.[31,32] In one study, 3 weeks after 20 mg/kg SI was injected into the tail vein of S6 mice, only subtle damage was observed in the retinal pigment epithelium layer in 29% (2/7) of mice in the absence of photoreceptor atrophy or outer retinal thinning.[31] In contrast, another study in B6 mice found significant retinal pigment epithelium atrophy and greatly reduced outer retinal thickness 1 week after 20 mg/kg SI injected into the orbital venous plexus; the incidence of damage was not reported.[32] It is possible that procedural differences between labs, such as the use of a different route of SI administration, affected outcomes. However, in a preliminary study, we confirmed the strain-dependent morphometric difference in susceptibility in response to SI. One week after IP injections of 20 mg/kg SI, retinal layer abnormalities were observed on OCT examination in the outer retina in 66% (2/3) of B6 mice compared to 25% (1/4) of SI-treated S6 mice (data not shown). These results supported the previous findings that B6 mice are more vulnerable to a systemic SI challenge than S6 mice.

In a conventional ex vivo assay, we tested and confirmed our working hypothesis that SI-treated B6 mice experience more outer retinal oxidative stress than SI-treated S6 mice (Fig. 1). These data raised the possibility that the differential response to SI occurred in the outer retina since the rod inner segment layer contains approximately 75% of retinal mitochondria (a major source of superoxide free radicals).[23,34] This

presumption was supported by the agreement between the ex vivo assay result and evidence for excessive outer retinal free radical production as measured by QUEST MRI (Figs. 1, 3, 4). QUEST MRI evaluates the total excessive free radical burden of the tissue because all species of free radicals are paramagnetic and ALA is a nonspecific free radical scavenger.[22,23,47,48] The present results (Figs. 1, 3, 4) provide first-time evidence supporting the use of spatial mapping of the 1/T1 difference between baseline and ALA treatment as a graded noninvasive index of severity of laminar-specific excessive free radical production.
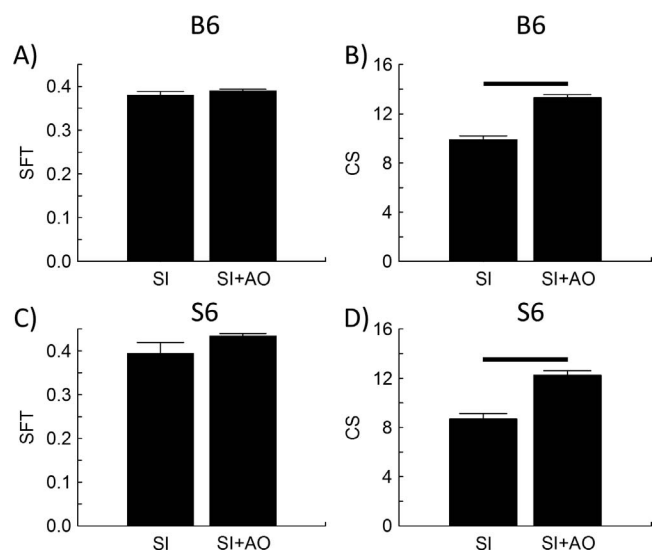

FIGURE 5. SI induced oxidative stress reduced contrast sensitivity but not acuity in both strains. Spatial frequency threshold (*left*) evaluated in B6 (*top row*) and S6 (*bottom row*) mice that were either SI-treated ($n = 10$, 4, respectively) or SI-treated+AO (IO3+AO, $n = 10$, 5, respectively). *Black bar*: significant difference ($P < 0.05$). *Error bars*: SEM.
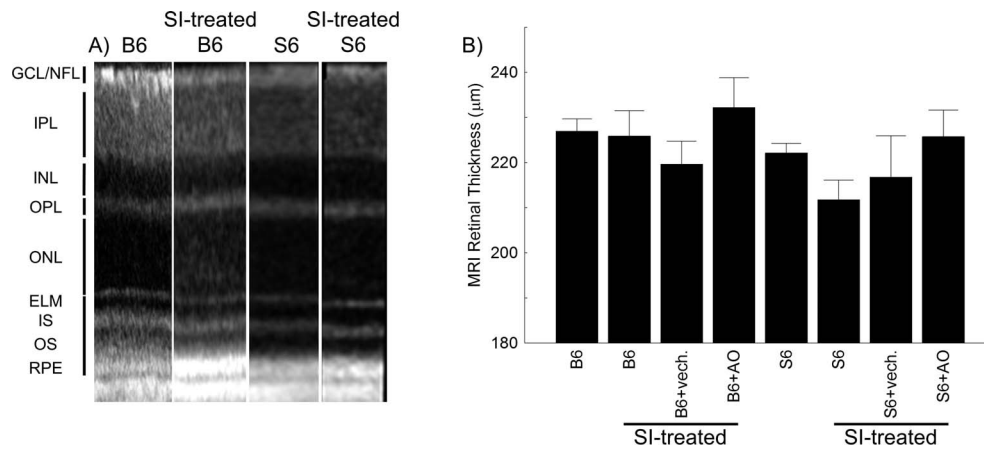
Figure 6. No evidence for retinal thinning due to SI-treatment in B6 and S6 mice. (**A**) Representative OCT images from untreated B6 (B6), SI-treated B6 (B6+IO3), untreated S6 (S6), and SI-treated S6 (S6+IO3) mice. RGC/NFL, retinal ganglion cell layer/nerve fiber layer; ELM, external limiting membrane; IS, inner segments of rod cells (ellipsoid region); OS, outer segments of rod cells; RPE, retinal pigment epithelium. (**B**) Representative MRI-derived whole retinal thicknesses for each group.

We also examined photopic OKT based on reports that indices of visual performance are sensitive to retinal oxidative stress (Fig. 5).[26–30,49] Our results were consistent with the idea of an oxidative stress response to SI in cone cells because photopic CS (but not SFT) is regulated by cone dopamine D4 receptors.[30,50,51] The OKT data also were consistent with a minimal oxidative stress response to SI in the inner retina, since SFT (but not contrast sensitivity) is modulated by dopamine D1 receptors in bipolar and horizontal cells of the inner retina, and was not responsive to AO treatment.[30,50,51] Together, these considerations raised the possibility that OKT measurements may be sensitive to layer-specific oxidative stress although more work clearly is needed to investigate the sensitivity of D1 and D4 receptor to oxidative stress.[26–30] Comparing the QUEST MRI and OKT results raises the novel possibility that rods exhibit oxidative stress before cone cells following SI treatment, although further studies are needed to address this point.

The molecular basis for the strain-dependent oxidative stress vulnerability to SI, and the spatially distinct responses within retinal layers of the outer retina, is not clear and was not the focus of this study. Nonetheless, we speculated that the strain-dependent differences in outer retinal oxidative stress might arise because S6 mice regenerate 11-*cis*-retinaldehyde faster than B6 mice due to different genetic forms of RPE65; systemic 11-*cis*-retinaldehyde recently was shown to reduce retinal oxidative stress and improve visual performance in experimental diabetic retinopathy.[19,27,52–54] However, other factors likely also differ between S6 and B6 mice and contribute to the observed results; more work in this area is needed to clarify the underlying mechanisms.[1,19,52–58]

In summary, our results highlighted QUEST MRI as a powerful, noninvasive, and graded measurement of excessive free radical production by neurons. QUEST MRI offers two major advantages. First, QUEST MRI uniquely and directly maps layer-specific regions generating excessive free radicals in contrast to the "grind and find" whole retinal assays ex vivo, and the behavioral OKT assay. Second, because QUEST MRI does not involve injection of a contrast agent, its translational potential into patients is high. In addition, our results supported and extended data in the literature that have suggested a genetic basis for outer retinal oxidative stress vulnerability.[17,20,26,33,59] Measuring retinal oxidative stress in vivo represents an important step in improving our ability to personalize AO treatment efficacy to slow progression, or possibly prevent, retinal degenerative diseases.

References

1. Organisciak DT, Vaughan DK. Retinal light damage: mechanisms and protection. *Prog Retin Eye Res*. 2010;29:113–134.

2. Sachdeva MM, Cano M, Handa JT. Nrf2 signaling is impaired in the aging RPE given an oxidative insult. *Exp Eye Res*. 2014; 119:111–114.

3. Oveson BC, Iwase T, Hackett SF, et al. Constituents of bile, bilirubin and TUDCA, protect against oxidative stress-induced retinal degeneration. *J Neurochem*. 2011;116:144–153.

4. Shen J, Yang X, Dong A, et al. Oxidative damage is a potential cause of cone cell death in retinitis pigmentosa. *J Cell Physiol*. 2005;203:457–464.

5. Sacchetti M, Mantelli F, Merlo D, Lambiase A. Systematic review of randomized clinical trials on safety and efficacy of pharmacological and nonpharmacological treatments for retinitis pigmentosa. *J Ophthalmol*. 2015;2015:737053.

6. Age-Related Eye Disease Study Research Group. A randomized, placebo-controlled, clinical trial of high-dose supplementation with vitamins C and E and beta carotene for age-related cataract and vision loss: AREDS Report No. 9. *Arch Ophthalmol*. 2001;119:1439–1452.

7. Campochiaro PA, Strauss RW, Lu L, et al. Is there excess oxidative stress and damage in eyes of patients with retinitis pigmentosa? *Antioxid Redox Signal*. 2015;23:643–648.

8. Punzo C, Xiong W, Cepko CL. Loss of daylight vision in retinal degeneration: are oxidative stress and metabolic dysregulation to blame? *J Biol Chem*. 2012;287:1642–1648.

9. Rohrer B, Pinto FR, Hulse KE, Lohr HR, Zhang L, Almeida JS. Multidestructive pathways triggered in photoreceptor cell death of the RD mouse as determined through gene expression profiling. *J Biol Chem*. 2004;279:41903–41910.

10. Sanz MM, Johnson LE, Ahuja S, Ekstrom PA, Romero J, van Veen T. Significant photoreceptor rescue by treatment with a combination of antioxidants in an animal model for retinal degeneration. *Neuroscience*. 2007;145:1120–1129.

11. Usui S, Komeima K, Lee SY, et al. Increased expression of catalase and superoxide dismutase 2 reduces cone cell death in retinitis pigmentosa. *Mol Ther*. 2009;17:778–786.

12. Komeima K, Rogers BS, Lu L, Campochiaro PA. Antioxidants reduce cone cell death in a model of retinitis pigmentosa. *Proc Natl Acad Sci U S A*. 2006;103:11300–11305.

13. Galbinur T, Obolensky A, Berenshtein E, et al. Effect of para-aminobenzoic acid on the course of retinal degeneration in the rd10 mouse. *J Ocul Pharmacol Ther*. 2009;25:475–482.

14. Berkowitz BA, Gradianu M, Bissig D, Kern TS, Roberts R. Retinal ion regulation in a mouse model of diabetic retinopathy: natural history and the effect of Cu/Zn Superoxide dismutase overexpression. *Invest Ophthalmol Vis Sci*. 2009;50:2351–2358.

15. Zheng L, Du Y, Miller C, et al. Critical role of inducible nitric oxide synthase in degeneration of retinal capillaries in mice with streptozotocin-induced diabetes. *Diabetologia*. 2007;50:1987–1996.

16. Berkowitz BA, Roberts R, Stemmler A, Luan H, Gradianu M. Impaired apparent ion demand in experimental diabetic retinopathy: correction by lipoic Acid. *Invest Ophthalmol Vis Sci*. 2007;48:4753–4758.

17. Cingolani C, Rogers B, Lu L, Kachi S, Shen J, Campochiaro PA. Retinal degeneration from oxidative damage. *Free Radic Biol Med*. 2006;40:660–669.

18. Danciger M, Yang H, Handschumacher L, LaVail MM. Constant light-induced retinal damage and the RPE65-MET450 variant: assessment of the NZW/LacJ mouse. *Mol Vis*. 2005;11:374–379.

19. Wenzel A, Remé CE, Williams TP, Hafezi F, Grimm C. The Rpe65 Leu450Met variation increases retinal resistance against light-induced degeneration by slowing rhodopsin regeneration. *J Neurosci*. 2001;21:53–58.

20. Lederman M, Hagbi-Levi S, Grunin M, et al. Degeneration modulates retinal response to transient exogenous oxidative injury. *PLoS One*. 2014;9:e87751.

21. Parmeggiani F, Sato G, De Nadai K, Romano MR, Binotto A, Costagliola C. Clinical and rehabilitative management of retinitis pigmentosa: up-to-date. *Curr Genom*. 2011;12:250–259.

22. Berkowitz BA, Lewin AS, Biswal MR, Bredell BX, Davis C, Roberts R. MRI of retinal free radical production with laminar resolution in vivo free radical production with laminar resolution in vivo. *Invest Ophthalmol Vis Sci*. 2016;57:577–585.

23. Berkowitz BA, Bredell BX, Davis C, Samardzija M, Grimm C, Roberts R. Measuring in vivo free radical production by the outer retina measuring retinal oxidative stress. *Invest Ophthalmol Vis Sci*. 2015;56:7931–7938.

24. Stinnett G, Moore K, Samuel E, et al. A novel assay for the in vivo detection of reactive oxygen species using MRI. In: *ISMRM 23rd Annual Meeting & Exhibition*. Toronto, Ontario: International Society for Magnetic Resonance in Medicine; 2015. Abstract 1917.

25. Matsumoto K-i, Hyodo F, Matsumoto A, et al. High-resolution mapping of tumor redox status by magnetic resonance imaging using nitroxides as redox-sensitive contrast agents. *Clin Cancer Res*. 2006;12:2455–2462.

26. Patel AK, Hackam AS. A novel protective role for the innate immunity Toll-Like Receptor 3 (TLR3) in the retina via Stat3. *Mol Cell Neurosci*. 2014;63:38–48.

27. Berkowitz BA, Kern TS, Bissig D, et al. Systemic retinaldehyde treatment corrects retinal oxidative stress, rod dysfunction, and impaired visual performance in diabetic micesystemic retinaldehyde treatment in diabetic mice. *Invest Ophthalmol Vis Sci*. 2015;56:6294–6303.

28. Franco LM, Zulliger R, Wolf-Schnurrbusch UE, et al. Decreased visual function after patchy loss of retinal pigment epithelium induced by low-dose sodium iodate. *Invest Ophthalmol Vis Sci*. 2009;50:4004–4010.

29. Cahill H, Nathans J. The optokinetic reflex as a tool for quantitative analyses of nervous system function in mice: application to genetic and drug-induced variation. *PLoS One*. 2008;3:e2055.

30. Jackson CR, Ruan GX, Aseem F, et al. Retinal dopamine mediates multiple dimensions of light-adapted vision. *J Neurosci*. 2012;32:9359–9368.

31. Zhou P, Kannan R, Spee C, Sreekumar PG, Dou G, Hinton DR. Protection of retina by αB crystallin in sodium iodate induced retinal degeneration. *PLoS One*. 2014;9:e98275.

32. Wang J, Iacovelli J, Spencer C, Saint-Geniez M. Direct effect of sodium iodate on neurosensory retina. *Invest Ophthalmol Vis Sci*. 2014;55:1941–1953.

33. Patel AK, Davis A, Rodriguez ME, Agron S, Hackam AS. Protective effects of a grape-supplemented diet in a mouse model of retinal degeneration. *Nutrition*. 2016;32:384–390.

34. Du Y, Veenstra A, Palczewski K, Kern TS. Photoreceptor cells are major contributors to diabetes-induced oxidative stress and local inflammation in the retina. *Proc Natl Acad Sci U S A*. 2013;110:16586–16591.

35. Santos JM, Tewari S, Kowluru RA. A compensatory mechanism protects retinal mitochondria from initial insult in diabetic retinopathy. *Free Rad Biol Med*. 2012;53:1729–1737.

36. Berkowitz BA, Grady EM, Khetarpal N, Patel A, Roberts R. Oxidative stress and light-evoked responses of the posterior segment in a mouse model of diabetic retinopathy. *Invest Ophthalmol Vis Sci*. 2015;56:606–615.

37. Packer L, Cadenas E. Lipoic acid: energy metabolism and redox regulation of transcription and cell signaling. *J Clin Biochem Nutr*. 2011;48:26–32.

38. Wen Y, Li W, Poteet EC, et al. Alternative mitochondrial electron transfer as a novel strategy for neuroprotection. *J Biol Chem*. 2011;286:16504–16515.

39. Poteet E, Winters A, Yan L-J, et al. Neuroprotective actions of methylene blue and its derivatives. *PLoS One*. 2012;7:e48279.

40. Berkowitz BA, Bissig D, Patel P, Bhatia A, Roberts R. Acute systemic 11-cis-retinal intervention improves abnormal outer retinal ion channel closure in diabetic mice. *Mol Vis*. 2012;18:372–376.

41. Douglas RM, Alam NM, Silver BD, McGill TJ, Tschetter WW, Prusky GT. Independent visual threshold measurements in the two eyes of freely moving rats and mice using a virtual-reality optokinetic system. *Vis Neurosci*. 2005;22:677–684.

42. Berkowitz BA, Grady EM, Roberts R. Confirming a prediction of the calcium hypothesis of photoreceptor aging in mice. *Neurobiol Aging*. 2014;35:1883–1891.

43. Berkowitz BA, Bissig D, Roberts R. MRI of rod cell compartment-specific function in disease and treatment in-ávivo. *Prog Retin Eye Res*. 2016;51:90–106.

44. Haacke EM, Brown RW, Thompson MR, Venkatesan R. *Magnetic Resonance Imaging: Physical Principles and Sequence Design*: New York: Wiley; 1999.

45. Bissig D, Berkowitz BA. Same-session functional assessment of rat retina and brain with manganese-enhanced MRI. *NeuroImage*. 2011;58:749–760.

46. Cheng H, Nair G, Walker TA, et al. Structural and functional MRI reveals multiple retinal layers. *Proc Natl Acad Sci U S A*. 2006;103:17525–17530.

47. Bakalova R, Georgieva E, Ivanova D, Zhelev Z, Aoki I, Saga T. Magnetic resonance imaging of mitochondrial dysfunction and metabolic activity, accompanied by overproduction of superoxide. *ACS Chemical Neurosci*. 2015;6:1922–1929.

48. Hyodo F, Murugesan R, Matsumoto Ki, et al. Monitoring redox-sensitive paramagnetic contrast agent by EPRI, OMRI and MRI. *J Magn Reson*. 2008;190:105–112.

49. Sen HA, Berkowitz BA, Ando N, de Juan E Jr. In vivo imaging of breakdown of the inner and outer blood-retinal barriers. *Invest Ophthalmol Vis Sci*. 1992;33:3507–3512.

50. Farshi P, Fyk-Kolodziej B, Krolewski DM, Walker PD, Ichinose T. Dopamine D1 receptor expression is bipolar cell type-specific in the mouse retina. *J Comp Neurol*. 2016;524:2059–2079.

51. Liu X, Grove JCR, Hirano AA, Brecha NC, Barnes S. Dopamine D1 receptor modulation of calcium channel currents in horizontal cells of mouse retina. *J Neurophysiol*. 2016;116:686–697.

52. Wenzel A, Grimm C, Samardzija M, Remé CE. The genetic modifier Rpe65Leu 450: effect on light damage susceptibility in c-Fos-deficient mice. *Invest Ophthalmol Vis Sci*. 2003;44:2798–2802.

53. Maeda A, Maeda T, Imanishi Y, et al. Retinol dehydrogenase (RDH12) protects photoreceptors from light-induced degeneration in mice. *J Biol Chem*. 2006;281:37697–37704.

54. Kolesnikov AV, Tang PH, Parker RO, Crouch RK, Kefalov VJ. The mammalian cone visual cycle promotes rapid M/L-cone pigment regeneration independently of the interphotoreceptor retinoid-binding protein. *J Neurosci*. 2011;31:7900–7909.

55. Balogh SA, McDowell CS, Stavnezer AJ, Denenberg VH. A behavioral and neuroanatomical assessment of an inbred substrain of 129 mice with behavioral comparisons to C57BL/6J mice. *Brain Res*. 1999;836:38–48.

56. Finn R, Kovács AD, Pearce DA. Altered sensitivity to excitotoxic cell death and glutamate receptor expression between two commonly studied mouse strains. *J Neurosci Res*. 2010;88:2648–2660.

57. Leo S, Straetemans R, D'Hooge R, Meert T. Differences in nociceptive behavioral performance between C57BL/6J, 129S6/SvEv, B6 129 F1 and NMRI mice. *Behav Brain Res*. 2008;190:233–242.

58. Mori MA, Liu M, Bezy O, et al. A systems biology approach identifies inflammatory abnormalities between mouse strains prior to development of metabolic disease. *Diabetes*. 2010;59:2960–2971.

59. Dong A, Shen J, Krause M, et al. Superoxide dismutase 1 protects retinal cells from oxidative damage. *J Cell Physiol*. 2006;208:516–526.

60. Berkowitz BA, Schmidt T, Podolsky RH, Roberts R. Melanopsin phototransduction contributes to light-evoked choroidal expansion and rod L-type calcium channel function in vivo melanopsin and choroid regulation. *Invest Ophthalmol Vis Sci*. 2016;57:5314–5319.